

Supporting information to:

Kinetic Monte Carlo simulation of the photodegradation process of polyester-urethane coatings

Koen N.S. Adema ^{a, b}, Hesam Makki ^{a, b}, Elias A.J.F. Peters ^a, Jozua Laven ^a, Leendert G.J. van der Ven ^a, Rolf A.T.M. van Benthem ^a, Gijsbertus de With^{*, a}

^a Eindhoven University of Technology, Laboratory of Materials and Interface Chemistry, Department of Chemical Engineering and Chemistry, P.O. Box 513, 5600 MB Eindhoven, The Netherlands

^b Dutch Polymer Institute (DPI), P.O. Box 902, 5600 AX Eindhoven, The Netherlands

* Corresponding author: G.deWith@tue.nl

Keywords:

Kinetic Monte Carlo; Simulation; Photodegradation; Polymer coating; Polyester-urethane.

S.I.-1: Implicit reaction-diffusion scheme for the oxygen concentration

As introduced in section 2.5, an implicit reaction-diffusion scheme for the concentration of oxygen in each cell is incorporated into the KMC scheme. Because all simulations were performed on single columns, oxygen diffusion is modelled as a 1-dimensional process in the thickness dimension.

For a column of N cells, labelled from 1 (top cell) to N (bottom cell), the oxygen concentration in each cell is considered at the (discretised) KMC-time right before and the time right after an update step. These times are denoted by t and $(t+1)$, respectively. The corresponding oxygen concentration vectors of the column are denoted as C^t and C^{t+1} , respectively. Diffusion is modelled as a Fickian process and the consumption due to oxidation reactions is described according to the rate equations from the KMC scheme. The oxidation rate of each individual radical j in cell i is given by

$$r_{j,i}[h^{-1}] = k_{ox}[m^3h^{-1}]N_jC_i[mol \cdot m^{-3}]N_{av}[mol^{-1}] \quad (1)$$

with N_{av} Avogadro's number, so that the total rate of oxidation R in cell i is given by

$$R_i[h^{-1}] = \sum_j r_{j,i} = k_{ox}C_iN_{av} \sum_j N_j \quad (2)$$

From the total oxidation rate in a cell, the effective oxidation rate constant k_{eff} in cell i is computed according to

$$k_{eff,i}[h^{-1}] = \frac{R_i}{C_iN_{av}V_{cell}} = \frac{k_{ox} \sum_j N_j}{V_{cell}} \quad (3)$$

This effective oxidation rate constant will be used to compute the reaction-term for oxygen in the reaction-diffusion scheme.

For each cell in the column, a stationary molar balance for the oxygen concentration at times t and $(t+1)$ can be constructed. For all cells that are not located at either of the two ends of the column, this molar balance is given by

$$(1 + k_{eff,i}t_{diff})C_i^{t+1} + P(2C_i^{t+1} - C_{i-1}^{t+1} - C_{i+1}^{t+1}) = C_i^t \quad (4)$$

with $P = D\Delta t_{diff}/(\Delta x)^2$ and Δx the distance between two cells in the thickness dimensions (which is equal to the cell height). Here an Euler backward time-integration and central differencing spatial discretization were used. For the two cells at the ends of the column ($i = 1$ and $i = N$), the molar balances read

$$(1 + k_{eff,1}t_{diff})C_1^{t+1} + P(3C_1^{t+1} - C_2^{t+1}) = C_1^t + 2PC_{sat} \quad \text{and} \quad (5)$$

$$(1 + k_{eff,N}t_{diff})C_N^{t+1} + P(C_N^{t+1} - C_{N-1}^{t+1}) = C_N^t \quad (6)$$

Equations (5) and (6) follow from the boundary conditions, that is, oxygen saturation at the surface of the column and a zero flux condition at the polymer-substrate interface. The molar balances for all cells together form a system of linear equations that can be written as a matrix equation that reads

$$\underline{A} C^{t+1} = C^t + 2P \begin{pmatrix} C_{sat} \\ 0 \\ \vdots \\ 0 \end{pmatrix} \quad (7)$$

with \underline{A} the tridiagonal reaction-diffusion matrix, given by

$$\underline{A} = \begin{pmatrix} 1 + k_{eff,1}t_{diff} + 3P & -P & 0 & \dots & 0 \\ -P & 1 + k_{eff,2}t_{diff} + 2P & \cdot & \cdot & \vdots \\ 0 & -P & \cdot & -P & 0 \\ \vdots & \cdot & \cdot & \cdot & -P \\ 0 & \dots & 0 & 1 + k_{eff,N-1}t_{diff} + 2P & -P \\ & & & -P & 1 + k_{eff,N}t_{diff} + P \end{pmatrix} \quad (8)$$

During the initialisation of the simulation, \underline{A} is constructed using the k_{eff} 's as calculated from equation (3), using the initial conditions for C^t . Next, equation (7) is solved for C^{t+1} . The updated oxygen concentration, which is considered constant during $0 \leq t_{sim} < t_{diff}$, is used to compute all individual oxidation rates according to equation (1). After these rates are set to the simulation, the KMC scheme is executed until $t_{sim} \geq t_{diff}$. Oxidation reactions may have occurred during this first simulation block, which means that the k_{eff} 's and thus (the reaction part of) \underline{A} should be updated. After performing those updates, equation (7) is solved again, of course using the C^{t+1} obtained from the previous iteration as the C^t of the present iteration (the previous “new concentration” is the present “old concentration”). The new C^{t+1}

that follows from solution of equation (7) is the oxygen concentration vector of the box during $t_{diff} \leq t_{sim} < 2t_{diff}$. This procedure is repeated until the simulation has been completed.

S.I.-2: Modelling photon absorption due to Weather-Ometer irradiation

As described in section 2.4, photon absorption is modelled as a property of the aromatic beads in the system and a distinction is made between monophenyls (absorptivity code 0) and biphenyls (absorptivity code 1), the latter absorbing a larger fraction of the incident flux. Analogous to the definition of absorbance in UV-VIS experiments, the absorbance can be defined in terms of simulation quantities as well. At any composition, the absorbance A of (a column of) cells can be written as

$$A(\lambda) = A_0(\lambda) + A_1(\lambda) = \frac{1}{O} [N_0 \sigma_0(\lambda) + N_1 \sigma_1(\lambda)] \quad (9)$$

where the labels 0 and 1 refer to the absorptivity code of the beads, and with σ the absorption cross-section [m^2], N the number of aromatic beads and O the irradiated cell (surface) area [m^2]. In the virgin material, all aromatic beads are monophenyls and $A = A_0$ because $N_1 = 0$. Values for $\sigma_0(\lambda)$ can be determined straightforwardly by comparing to the experimental absorptivity $\alpha_0(\lambda)$. Values for $\sigma_1(\lambda)$, however, cannot be determined *a priori*. The reason is that, even though the absorptivity and thus the absorbance of the degraded phase are known from the experimental reference, the ratio $[N_1/N_0]$ during exposure is not known, as no peak in the IR spectrum could be identified to make this distinction possible. The fact that $\sigma_1(\lambda)$ is an unknown quantity has consequences for handling the polychromaticity of WOM exposure. If the fully detailed spectra are used, say, discretised in packages of a 1 nm spectral width, an unknown value of σ_1 for each package is required, which means that the number of unknown parameters blows up very quickly. Therefore, it is more reliable to split up the wavelength range into as few as possible ranges to keep the number of σ_1 -parameters minimal.

Because the reason for the split-up is to incorporate the effect of different penetration

depths, it makes sense to base the choices for this split-up on the penetration depth spectrum.

Fig. 1 shows the penetration depth spectrum corresponding to 5% transmittance for a virgin coating and for degraded material.

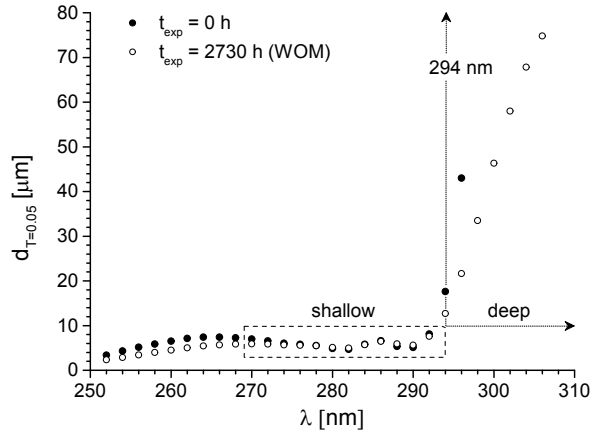


Fig. 1: Penetration depth spectrum corresponding to 5% transmittance for a virgin coating (solid symbols) and for degraded material after 2730 h of WOM exposure (open symbols).

From this figure, it can be seen that the penetration depth for both virgin and degraded material does not vary too much for wavelengths below roughly 294 nm and then starts to increase rapidly with increasing wavelength. Due to this behaviour, it was decided to split the spectral dependence for the simulations into two regimes: a regime of photons of up to 294 nm wavelength, that penetrate only shallowly into the coating (typically 4-8 μm) and a regime above 294 nm wavelength that contains photons that practically penetrate all the way through. Placing this boundary at 294 nm has an additional advantage for simulating WOM degradation. From the calculations in the experimental reference, it was found that the absorbance in the regime $270 < \lambda < 294 \text{ nm}$ is practically unchanged during WOM-degradation. Because the total number of aromatic beads ($N_0 + N_1$) is kept constant in the simulation, this means that for the short-wavelength regime $\sigma_1 = \sigma_0$ and hence there is only one unknown σ_1 -parameter required for the simulation input (that is, the σ_1 of the long-wavelength regime).

The absorption of photons during exposure is determined by the overlap of the surface

irradiance spectrum with the absorption cross-section spectrum. The effective absorption obtained by these two quantities, integrated over any wavelength range $[\lambda_1, \lambda_2]$, is defined as

$$\phi_{eff} \cdot \sigma_{eff} = \int_{\lambda_1}^{\lambda_2} d\lambda \Phi(\lambda) [N_0 \sigma_0(\lambda) + N_1 \sigma_1(\lambda)] \quad (10)$$

The effective surface irradiance ϕ_{eff} is now chosen to represent a quantity that does not depend on the changing absorptive properties of the coating during degradation, by defining

$$\phi_{eff} = \int_{\lambda_1}^{\lambda_2} d\lambda \Phi(\lambda) \quad (11)$$

so that ϕ_{eff} can be calculated directly from the surface irradiance spectrum $\Phi(\lambda)$ [$\text{m}^{-2}\text{s}^{-1}\text{nm}^{-1}$] and represents the effective photon flux that enters the coating (top layer of cells in the box).

From equations (10) and (11), it then follows that σ_{eff} can be written as

$$\sigma_{eff} = \frac{\int_{\lambda_1}^{\lambda_2} d\lambda \Phi(\lambda) [N_0 \sigma_0(\lambda) + N_1 \sigma_1(\lambda)]}{\int_{\lambda_1}^{\lambda_2} d\lambda \Phi(\lambda)} \equiv N_0 \sigma_{0,eff} + N_1 \sigma_{1,eff} \quad (12)$$

and thus that each individual $\sigma_{i,eff}$ is given by

$$\sigma_{i,eff} = \frac{\int_{\lambda_1}^{\lambda_2} d\lambda \Phi(\lambda) \sigma_i(\lambda)}{\int_{\lambda_1}^{\lambda_2} d\lambda \Phi(\lambda)} \quad (13)$$

From the definition of the absorbance in equation (9), the relation between the monophenyl absorption cross-section and the absorptivity of the virgin coating ($N_1 = 0$) can be established as

$$\sigma_0(\lambda) = \frac{V}{N_0} \alpha_0(\lambda) = \frac{1}{\rho_0} \alpha_0(\lambda) \quad (14)$$

which means that $\sigma_{0,eff}$ can be calculated from $\alpha_0(\lambda)$ by insertion of equation (14) into equation (13). Because the biphenyl absorption cross-section spectrum ($\sigma_1(\lambda)$) is not known, $\sigma_{1,eff}$ cannot be calculated beforehand, but is a simulation variable instead.

For the simulation of WOM exposure, the spectral dependence is split into two regimes, that is, the short wavelengths (270-294 nm), labelled ‘‘S’’ and the long wavelengths (294-334 nm), labelled ‘‘L’’. The upper limit for the long-wavelength regime is based on the outcome of the kinetic model for photolysis from the experimental reference.

S.I.-3: Parameter optimisation based on singular value decomposition

An ideal match between simulation and experiment via the optimised set of parameters [P_{opt}] corresponds mathematically to

$$O(x) = E \quad (15)$$

with O a vector of simulated observables, E a vector with the corresponding experimental quantities and x a vector with the (logarithms of) simulation input parameters. The solution of equation (15) can be iteratively found by means of the Newton-Raphson method. Suppose we have a guess of the parameter-vector at iteration k , that is, x^k then for the next iteration we would like to have $O(x^{k+1}) = E$. By linearization one obtains,

$$O_j(x^k) + \sum_i \frac{\partial O_j(x^k)}{\partial x_i} (x_i^{k+1} - x_i^k) = E_j \quad or \quad (16)$$

$$O(x^k) + J \Delta x = E \quad (17)$$

as the derivative term in this equation is a matrix element J_{ji} of the Jacobian matrix J . The elements of this Jacobian matrix have already been obtained for the case of 5 observables O_j and the 15 parameters $x_i = \ln p_i$ from Fig. 8, because they are equal to the total length of each vertical bar (the $+R$ and $-R$ together). Exact solution of equation (17) requires inversion of the Jacobian, but because this Jacobian matrix is non-square, this is impossible by definition.

Therefore a method known as singular value decomposition is used. In short, the Jacobian matrix, sized m-by-n, is decomposed in such a way that

$$J = \underline{U} \underline{S} \underline{V}^T \quad (18)$$

with \underline{S} a diagonal matrix (m-by-n) and with \underline{U} (m-by-m) and \underline{V} (n-by-n) unitary matrices, also called orthogonal matrices when all their elements are real. By combining this decomposed definition with equation (17), one can write the matrix equation

$$\underline{S} Z = R \quad (19)$$

with $Z = \underline{V}^T \Delta x$ and $R = \underline{U}^T (E - O)$. The idea is now to solve equation (19) with the constraint that the change in x and thus $|Z|^2$ is kept small, so that the optimal solution is approached via small steps through the parameter space, minimising the risk of ending up with unphysical results. When $n > m$ (more parameters than observables), which is the case here, the diagonal matrix \underline{S} only contains n nonzero elements, that is $[S_{11}, \dots, S_{mm}]$, which means that only $[Z_1, \dots, Z_n]$ influence the solution of equation (19). Each of these n terms contributes to $|Z|^2$ with a magnitude R_j/S_{jj} , so that terms with a relatively small S_{jj} have a relatively large influence on $|Z|^2$ and potentially only introduce noise into the solution algorithm. Therefore it is often better to neglect those terms, that is, to set the corresponding Z_j terms to 0, in order to arrive at the best possible solution.

The optimisation procedure just described was performed by constructing a Jacobian that contains the high and medium-influence responses from Fig. 8 (solid and dashed ellipses) for the seven primary rate constants and the four other parameters from Table 4. After singular value decomposition of this Jacobian, it turned out that two terms from the diagonal matrix (S_{44} and S_{55}) were relatively small compared to the other terms and so the corresponding terms Z_4 and Z_5 were set to 0. Using the three remaining terms, new parameter sets were found iteratively from solving $\Delta x = \underline{V} Z$ and re-running the simulation with the new parameter set until convergence, which occurred within typically four iterations. The final result of this

procedure is the optimised parameter set [P_{opt}]. Because of their insignificant influence on the five observables used for the optimisation procedure, the four secondary rate constants from Table 4 could not be optimised and hence their initially guessed values are reported in that table and were used in all simulations in this article.